Bagraev NT, et al., J Altern Complement Integr Med 2020, 6: 112
DOI: 10.24966/ACIM-7562/100112

HSOA Journal of Alternative, Complementary & Integrative Medicine

Research Article

Prospects for THz Therapy: Effective treatment of Affections Caused by COVID-19

NT Bagraev[1,2,3]*, PA Golovin[3], VS Khromov[1], LE Klyachkin[1,2], AM Malyarenko[1,2], VA Mashkov[3], BA Novikov[2], AP Presnukhina[4], AS Reukov[4] and KB Taranets[3]

[1]*Ioffe Institute, St. Petersburg, Russia*

[2]*Dipole Structures LLC, St. Petersburg, Russia*

[3]*Peter the Great St. Petersburg Polytechnic University, St. Petersburg, Russia*

[4]*Almazov National Medical Research Centre, St. Petersburg, Russia*

Abstract

The characteristics of Terahertz (THz) irradiation generated by a Silicon Nanosandwich Structure (SNS) under the conditions of a stabilized drain - source current are demonstrated. The frequency of irradiation arising from the quantum Faraday Effect is determined by the parameters of micro cavities embedded in the edge channels of a silicon nanosandwich structure confined by the negative-U centers. The obtained characteristics of a compact THz irradiation source determine the basis for highly effective medical applications.

For confirmation, the results of highly effective treatment of patients with pulmonary pathologies, including pathology caused by a new type of coronavirus infection, are presented. It was shown that the early (in the first day) use of THz irradiation made it possible to reduce the patient's stay in the intensive care unit, as well as the time of patient intubation and stay on mechanical ventilation, to reduce the radiological and pharmacological load on the patient, to increase the chances of a favorable prognosis in patients with risk factors.

Also, we present the first findings on the resonance response of living bio-tissue to the THz irradiation that allow their identification by measuring the changes of the longitudinal conductance and the lateral voltage within frameworks of the SNS prepared in the Hall geometry. The mechanism of the THz response is discussed, with the model of the Shapiro steps related generation. The THz resonance response from living bio-tissue under the THz irradiation is also applied to the definition of oncological breast disease, because recent studies in the field of THz diagnosis showed that there is a difference between spectral characteristics of normal and cancerous cells. Therefore, promising is to use sources and recorders of the THz irradiation for an early diagnosis of breast disease.

Keywords: Coronavirus infection; Negative-U centers; Pulmonary pathologies; Silicon nanosandwich structure; THz diagnosis for oncological breast disease; Terahertz irradiation

Introduction

In recent years, studies of materials and nanostructures based on them, which make it possible to detect macroscopic quantum effects at high temperatures up to the room temperature, have been of great interest [1-7]. One of the main conditions for revealing these effects is the effective neutralization of electron - electron interaction in the edge channels of nanostructures. For this reason, the high-temperature Shubnikov - de Haas, de Haas - van Alphen oscillations, the Hall resistance quantum staircase, and the longitudinal conductance quantum staircase were observed in graphene, in a number of related topological insulators and superconductors [2,3], as well as in silicon, 6H-SiC and CdF_2 nanostructures, in which the edge channels are confined by the chains of the negative-U centers [4-7]. It should be noted that the neutralization of the electron - electron interaction in the edge channels is also predicted when they are confined by the chains of d- or f-elements [8,9]. But, the coatings consisting of the negative-U centers appear to contribute more effectively to the observation of macroscopic quantum phenomena at high temperatures [4-7]. Moreover, among the observed macroscopic quantum phenomena, the quantum Faraday Effect takes the important part, which, as it was found, gives rise to the capture of the single magnetic flux quanta to the edge channels containing single carriers, thereby emitting irradiation in the THz- and GHz frequency range depending on edge channels length [4,6]. It was shown that it is possible to control the frequency and amplitude characteristics not only by varying the dimensional parameters of the edge channels, but also by incorporating various micro cavity systems into them [5-7]. Thus, various versions of compact terahertz irradiation sources were developed, which are widely used in practical medicine [10].

Currently, some practical and scientific experience has been accumulated in the use of the THz irradiation in burn disease, strokes, diabetes mellitus, joint diseases, degenerative-dystrophic lesions of the spine, and in the maintenance of patients with a cardiac surgical profile. The use of the THz irradiation from the SNS devices was successfully tested at hospitals of St. Petersburg and Moscow (1995-2020). It should be noted that no side effects were noted. Even in the most severe clinical conditions (shock states in burn disease, states of oppressed consciousness and motor disorders in strokes, psychomotor arousal, encephalopathy, pain syndrome in generalized herpetic

***Corresponding author:** NT Bagraev, Ioffe Institute, Dipole Structures LLC, St. Petersburg, Russia, E-mail: bagraev@mail.ioffe.ru; nikolay.bagraev@gmail.com

Citation: Bagraev NT, Golovin PA, Khromov VS, Klyachkin LE, Malyarenko AM, et al. (2020) Prospects for THz Therapy: Effective treatment of Affections Caused by COVID-19. J Altern Complement Integr Med 6: 112.

Received: July 29, 2020; **Accepted:** August 01, 2020; **Published:** August 08, 2020

ganglionitis and polyneuropathies in diabetes mellitus, degenerative-dystrophic changes in the spine and rheumatoid polyarthritis) use of the THz irradiation.

Thus, the indications for the use of the THz devices based on the SNS nanostructures are:

- Treatment of thermal and other skin lesions in combination with anti-shock effects
- Accelerated healing of wounds, bed and trophic ulcers of large area, treatment of postoperative scar deformities
- Treatment of skin and wound lesions in case of radiation lesions
- Treatment of diseases of the immune system
- Treatment of severe spinal injuries and prevention of musculo-skeletal diseases
- Treatment of angeopathy in diabetes mellitus
- Treatment of various types of arthrosis, prevention and treatment of complications arising from rheumatoid arthritis
- Hypotension treatment
- Treatment of pulmonological diseases
- Maxillofacial surgery in the treatment of scar deformities on the face
- Treatment of uncomplicated and chronic gastric and duodenal ulcers
- Therapy after surgical operations in conditions of withdrawal from anesthesia
- Anti-shock therapy in the mobile version of Ambulance
- Prevention and treatment of sports injury
- Health treatments

In addition, according to the latest data, the plant can be effectively used to treat severe forms of demyelinating diseases of the central nervous system.

It should be noted that terahertz irradiation is becoming more widespread in world therapeutic practice [11]. Moreover, the far-IR and THz range includes irradiation with a wavelength of 10 to 1000 μm, respectively, with a frequency of 300 GHz to 30 THz, therefore a specific frequency or wavelength is usually indicated for its unambiguous characteristic. Besides, the combination of GHz, THz and IR radiation is of the greatest interest for the direct therapeutic effect on biological tissues, because the IR irradiation can stimulate the most important biochemical reactions in the human body, while the THz component of the irradiation provides a resonant increase of this effect due to the bonds "shaking" in protein molecules [10], and GHz modulation affects the longitudinal vibrations of the DNA - oligonucleotides [5,7]. The frequency selection of the THZ irradiation from the SNS nanostructures allows one of the more significant practical challenges currently occupying molecular biologists is to find better ways of identifying short strands of DNA. Called oligonucleotides, these strands of nucleotides are hugely useful in processes such as genetic testing, forensics and DNA amplification [12]. In addition to the above, the THz frequency selection of the DNA oligonucleotides seems to be an important step for the implementation of personalized medicine in the treatment of severe genetic diseases.

This combination of modulating frequencies can be implemented in exactly the same way as the principle of synchronous detection widely used in radio engineering in the range of radio waves, in which the short-wave radiation (high frequency) is modulated by the long-wave radiation (low frequency). It is clear that in the case of the optical wavelength range, the shorter THz irradiation should be modulated by the longer wavelength GHz irradiation. The advantages of such a symbiosis are obvious, but until recently, the technical implementation of sources with similar characteristics was practically impossible. However, the developed compact sources of the THz irradiation from the edge channels of silicon nanostructures made it possible to create a broadband THz emitter operating in the wavelength range of 1-700 μm with THz modulation (40 GHz - 3.5 THz) in the entire irradiation spectrum [10]. As noted above, this emitter is used in various fields of practical medicine with a high therapeutic effect, which is demonstrated in this article by the example of the highly effective treatment results of patients with pulmonary pathologies, including pathology caused by coronavirus. Also, we present the first findings on the resonance response of living bio-tissue to the THz irradiation that allow their identification by measuring the changes of the longitudinal conductance and the lateral voltage within frameworks of the SNS prepared in the Hall geometry. The mechanism of the THz response is discussed, with the model of the Shapiro steps related generation. The THz resonance response from living bio-tissue under the THz irradiation is also applied to the definition of oncological breast disease, because recent studies in the field of THz diagnosis showed that there is a difference between spectral characteristics of normal and cancerous cells [1]. Therefore, promising is to use sources and recorders of the THz irradiation for an early diagnosis of breast disease.

Silicon source of THz Irradiation

A silicon nanostructure is a Silicon Nanosandwich (SNS) that represents an ultra-narrow p-type Silicon Quantum Well (p-Si-QW) confined by δ-barriers heavily doped with boron (5×10^{21} cm^{-3}) on the n-Si (100) surface (Figure 1) [4,6]. SNS are formed within the framework of the Hall geometry in the process of preliminary oxidation and subsequent short-time diffusion of boron from the gas phase [4,6]. It was shown that boron atoms in the δ-barriers align crystallographically oriented sequences of the negative-U trigonal dipole centers (B^+ - B^-), which are formed as a result of the negative-U reaction: $2B_o \rightarrow B^+ + B^-$ [4,6]. It was found that the presence of the negative-U dipole boron centers quenches the electron-electron interaction, thereby allowing the macroscopic quantum phenomena at high temperatures, up to the room temperature [4,6]. Moreover, the most effective quenching of the electron-electron interaction is achieved in the edge channels of the quantum well confined by the negative-U dipole boron centers. It should be noted that the magnitude of the negative correlation energy is determined by the degree of the interplay of the electron-vibrational interaction and the charge correlations and is revealed by the appearance of a local phonon mode [4,6]. Detailed studies of the conductivity angular dependences made it possible to determine the value of the negative correlation energy for the dipole boron centers, 0.044 eV, which demonstrates the possibility of observing macroscopic quantum phenomena at high temperatures.

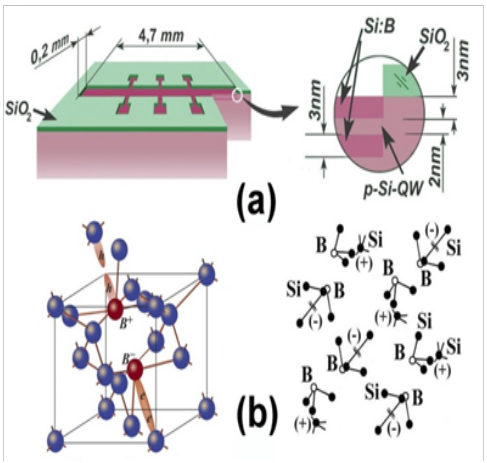

Figure 1: (a) Design of SNS with typical dimensions. (b) The dipole trigonal center of boron (B+ - B-) with the negative-U energy and the chains of boron dipole centers in the δ - barriers confining p-Si-QW.

As a result of the effective neutralization of the electron-electron interaction, the holes located inside the edge channels form the chains of the quantum harmonic oscillators generating Terahertz (THz) and Gigahertz (GHz) irradiation due to the Faraday quantum effect under conditions of stabilized drain-source current flowing along edge channels of the SNS, which induces the appearance of a magnetic field. In turn, the emerging magnetic flux quanta, h/2e, (magnetic field lines) are captured on segments of the edge channels (pixels) containing single holes because of the neutralization of the electron-electron interaction and, as a result of the Faraday effect, induce a current in the pixels, which leads to the THz and GHz generation: $I_{ind}\,\Delta\Phi = E(h\nu)$, where: $\Delta\Phi_{=}\,\Phi_{0=}\,h/2e$. Depending on the value of the stabilized drain – source current, two THz generation mechanisms are possible [5,7,10]. At low currents (<9 10^{-7}A), the above mechanism dominates, arising from the generation of current in pixels during the capture of single magnetic flux quanta. For currents much higher than the above value, the generation of the THz irradiation occurs similarly to a frame bounded by two back-to-back Josephson junctions. In this case, the generation frequency is determined from the known relation: $h\nu=2e\,I_{ind}R$, where $R = h/2e^2$ - the quantum of resistance corresponds to a pixel with a single hole. Taking into account the density value of two-dimensional holes in the used SNS structures, 3 10^{13} m^{-2}, the sizes of pixels with a single hole correspond to 16.6 μm x 2 nm, which, in turn, leads to the predominant generation of the THz irradiation with a frequency of 2.8 THz.

Accordingly, in the presence of micro cavities with sizes that are consistent with the sizes of the pixels or their groups that are built into the edge channels, the THz irradiation power can increase significantly. In addition, by varying the parameters of the micro resonators embedded in the SNS edge channels in the presence of negative-U centers, it is possible to select the THz generation frequency [4-7].

Thus, the characteristics of the built-in micro cavities determine the shape of the THz emission spectra corresponding to one or another frequency range of the electromagnetic spectrum. For example, as noted above, in order to obtain effective radiation with the frequency of 2.8 THz, which is extremely important for the purposes of biology and practical medicine [13-15], it is necessary, in accordance with the sizes of the pixels containing single holes, to insert micro cavities with a size of 16.6 μm into the edge channels, the presence of which is reflected in the electroluminescence spectra as the Rabi splitting (Figure 2) [5].

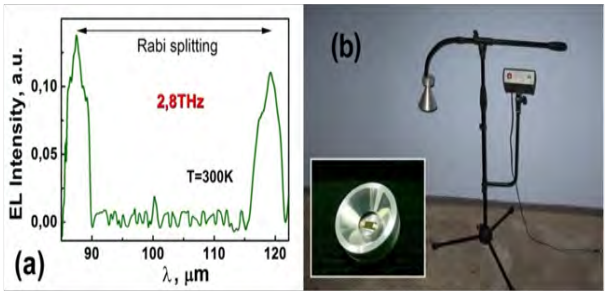

Figure 2: (a) Electroluminescence spectrum of SNS with embedded micro cavities, demonstrating the contribution of a micro cavity with a characteristic size of 16.6 μm as the Rabi splitting under the conditions of the THz generation by a quantum harmonic oscillator at the frequency of 2.8 THz, which is extremely important for biology and practical medicine. I_{ds} = 30 mA. (b) the "IR-Dipole" therapeutic equipment for IR and THz therapy; the IR-THz emitter used in the apparatus is shown in the insert.

Manufactured in accordance with the principles described above, compact THz emitters are the basic elements of the "IR-Dipole" (Figure 2) and "Infrateratron" therapeutic equipment, which is successfully used in the treatment of a number of socially significant diseases [10]. The full spectrum of the THz irradiation generated by this equipment under the conditions of a stabilized drain – source current flowing through the SNS is shown in Figure 3.

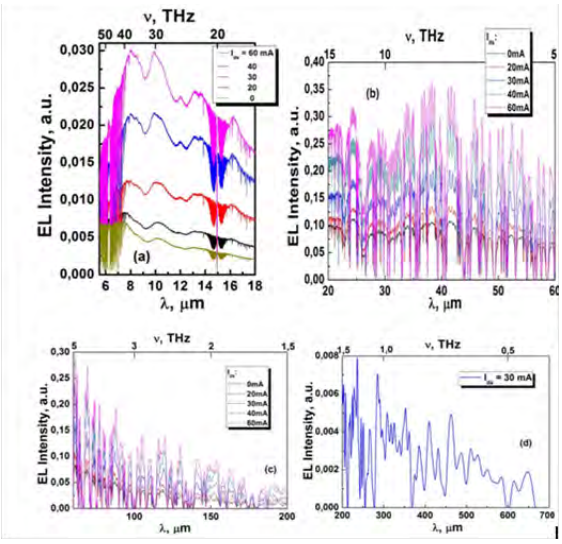

Figure 3: The full spectra of THz irradiation generated by the therapeutic equipment "IR-Dipole" and "Infrateratron" at various operating currents. Spectra obtained using IR-Fourier spectrometer Bruker-Physik VERTEX 70.

The Use of THz Irradiation in Pulmonology

One of the important applications of the created "IR-Dipole" apparatus is practice in cardiac surgery to eliminate early pulmonary complications after surgery, for example, after aortocoronary bypass

surgery [16]. It should be noted, that the development of pulmonary complications aggravates the condition of cardio surgical patients, requires additional therapeutic and diagnostic measurements, increases the pharmacological load, lengthens the length of hospital stay and can lead to death. The effectiveness of the THz irradiation generated by the IR-Dipole apparatus for the treatment of patients with pulmonary pathologies was analyzed in detail at the VA Almazov National Medical Research Center (St. Petersburg). The goal of this work is to study the development of Nosocomial Pneumonia (NP) and Ventilator-Associated Pneumonia (VAP) in patients in the early stages after cardiac surgery.

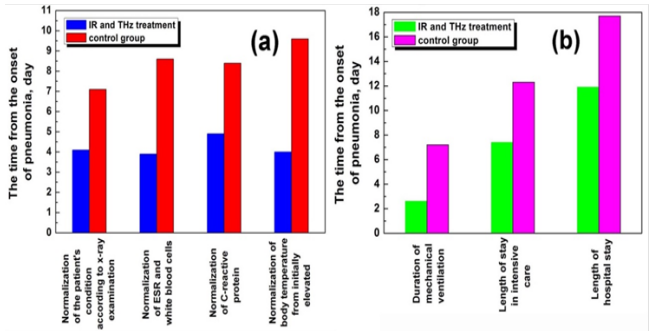

Figure 4: The effectiveness of the THz irradiation practice for the treatment of pneumonia.

An observational retrospective open comparative study with pseudo-control ("case-control") was conducted on the basis of the resuscitation department of cardiovascular surgery, which received patients after coronary artery bypass grafting and / or heart valve prosthetics. The study included patients with advanced complications in the form of focal infiltrative changes in the lungs (NP and VAP). Two groups were distinguished: the group in which, in addition to drug therapy, the exposure to the THz irradiation using the IR-Dipole apparatus on the Da-bao acupuncture point (RP 21) was performed, and the control group, which received standard treatment.

The early (on the first day) use of the THz irradiation allowed: to reduce the patient's stay in the intensive care unit by 4-8 days; reduce radiological and pharmacological burden on the patient; reduce the time of intubation of the patient and finding him on mechanical ventilation by 4-8 days; increase the chances of a favorable prognosis in patients with risk factors; start rehabilitation measures 4-8 days earlier. The comparative analysis of the effectiveness of the IR-Dipole apparatus for the treatment of pneumonia of different etiologies is given in figure 4.

The efficiency of using the THz irradiation is illustrated by the following clinical example. The patient is 64 years old. Diagnosis: Coronary heart disease. Atherosclerosis of the coronary arteries. Angina pectoris. Hypertonic disease. Operation 06/06/2012: sternotomy, mammary coronary artery bypass grafting, vein graft to the obtuse marginal artery, diagonal artery, right coronary artery, with cardiopulmonary bypass and blood cardioplegia. 06/06/12 intraoperatively - a drop in hemodynamics, ventricular fibrillation. Resuscitation measures were carried out. The main stage of the operation had no features. The postoperative course is extremely severe, with cardiovascular and respiratory failure, metabolic disorders, pneumonia, and a septic state. From 06/10/12 to 06/15/12 was on mechanical ventilation. 06/13/12 Clinical, laboratory, and radiological signs of bilateral lower-lobe pneumonia appeared. 06/13/12 antibiotic therapy has been started (according to the generally accepted scheme). During the discussion at the consultation, the THz-physiotherapy using the IR-Dipole device was added to the treatment. A change in key blood parameters during the treatment of pneumonia with the THz irradiation is presented in the table 1.

	ESR mm/h (normal 2-20)	RBS 1012 1/L (normal 4-5)	WBS 109 1/L (normal 4-9)
Before treatment	41	3.66	28.7
2 days later	19	3.62	8.9
7 days later	10	4.10	8.7

Table 1: A clinical example of a change in key blood parameters during the treatment of pneumonia with the THz irradiation.

The Use of THz Radiation for a New Type of Coronavirus Infection Complicated by Pneumonia

In this study, 12 patients aged 44 to 67 years with diagnoses U07.1 + J12.8 were dynamically observed in the early rehabilitation period at the inpatient stage. Patients, residents of St. Petersburg, were hospitalized in medical institutions of the city with signs of respiratory failure, dry cough, weakness and hyperthermia. After hospitalization, the diagnosis "COVID-19, virus identified" (code U07.1 - https://icd.who.int/browse10/2019/en#/U07.1) was confirmed. According to the results of computed tomography (CT), according to the indicators of clinical and biochemical blood tests (with markers of inflammatory processes), the diagnosis was clarified and supplemented with community-acquired bilateral polysegmental pneumonia and first-degree respiratory failure (another viral pneumonia - code J12.8 - https://icd.who.int/browse10/2019/en#/J12.8) as a complication of the main one.

Patients examined taking into account age, gender, main diagnosis, complications and clinical symptoms were divided into two groups compared according to these parameters: the main group (MG) and the Control Group (CG). Patients in both groups received antibacterial, anti-inflammatory, symptomatic, antiviral and gastro protective therapy. In addition to the pharmacotherapy in the early rehabilitation period, patients with OG underwent a course of THz-therapy using the "IR-Dipole" apparatus in the amount of 10-12 procedures until they were discharged from the hospital. Patients of both groups, 6 people in each (3 men and 3 women) were hospitalized 3-5 days after deterioration. They had no history of thyroid disease or changes characteristic of the pathology of this organ revealed during the examination. The main comorbidities in the group were degenerative-dystrophic diseases of the spine (DSD) without clinical symptoms requiring drug treatment. All patients had no bad habits. According to CT data, all examined patients had multiple extensive merging foci of irregular-shaped infiltration of the "ground glass" type in all segments of both lungs. The total lesion volume exceeded 50%. The data of clinical and laboratory blood parameters in the groups are presented in tables 2-4.

Indications for starting the use of THz radiation in the early rehabilitation period were the absence of deterioration (stabilization) of clinical symptoms, improvement of clinical and laboratory

parameters of blood and urine. The assessment of such physiological parameters as appetite, sleep, urine output and defecation of patients was also taken into account. Subjective symptoms were also taken into account: mood, presence or absence of weakness, headaches, dizziness, performance. Subjective symptoms were assessed using a 10-point Robson scale (increase with increasing value). The results are shown in the table 5.

Blood indicators	Before the 1st procedure		After the 4th procedure		After the 10th procedure	
	Min	Max	Min	Max	Min	Max
WBC (10^9/L)	11.7	19.4	7.7	10.4	5.9	9.7
LYM (%)	12.3	17.0	15.6	23.4	16.8	26.2
PLT (10^9/L)	211000	312000	236000	352000	250000	375000
ESR (мм/h)	56	69	33	46	10	23
hs-CRP (мg/dL)	28.0	37.0	14.0	20.4	0.3	1.0
AST (1/L)	70	95	46	67	21	40
ALT(1/L)	96	118	52	76	27	48
S-Fer (ng/mL)	1408	2463.5	759	1331.8	352	515.8
GLU(mmol/L)	7.1	8.3	5.0	6.2	4.5	5.8

Table 2: Clinical blood parameters before the 1st, after the 4th and 10th THz irradiation procedures in the MG.

Blood indicators	The day corresponding to the 1st THz irradiation procedures in the MG		The day corresponding to the 4th THz irradiation procedures in the MG		The day corresponding to the 10th THz irradiation procedures in the MG	
	Min	Max	Min	Max	Min	Max
WBC (10^9/L)	11.6	19,3	9.1	15.7	6.7	12.1
LYM (%)	12.0	16.8	14.6	18.1	15.8	19.0
PLT (10^9/L)	215000	310000	217000	338000	219000	360000
ESR (мм/h)	55	69	35	53	15	36
hs-CRP (мg/dL)	29.0	36.0	15.3	21.6	1.2	3.8
AST (1/L)	68	94	51	71	33	52
ALT(1/L)	98	112	64	87	49	71
S-Fer (ng/mL)	1399.5	2465.0	780.0	1427.0	401.5	717.5
GLU(mmol/L)	7.0	8.2	6.1	7.4	5.2	6.6

Table 3: Clinical blood parameters of the CG patients on the days corresponding to the 1st, the 4th and 10th THz irradiation procedures in the MG.

*Robson scale:
https://worldwide.espacenet.com/publicationDetails/biblio?CC=GB&NR=2049431&KC=&FT=E&locale=en_EP]

During THz-therapy, we used a test for monitoring the Temperature of Acupuncture Points (MTAP), which is successfully used in the treatment of VAP in cardiac surgery patients. With the help of a non-contact infrared thermometer, the temperature of the skin surface is measured in the projection of the epicenter of a set of representative acupuncture points, which makes it possible to make the right choice of the irradiation zone using the IR-Dipole apparatus to increase the effectiveness of the therapy.

In the case of COVID-19 with pneumonia complication, additional representative acupuncture points (AP) were identified in addition to the basic set of temperature measurement points: Qishe (E11 / St11) (paired) and Tiantu (VC22) (Figure 5). These points are used in reflexology in the treatment of cough, shortness of breath, purulent sputum, bronchitis, thyroid diseases and lung diseases. Since all patients in this group of thyroid problems were not diagnosed, the temperature monitoring of the AP data will reflect the state of the rehabilitation process in COVID-19 with complications in the form of pneumonia.

Blood indicators	The day corresponding to the 1st THz irradiation procedures in the MG		The day corresponding to the 4th THz irradiation procedures in the MG		The day corresponding to the 10th THz irradiation procedures in the MG	
	Min	Max	Min	Max	Min	Max
WBC (10^9/L)	15.6	15.5	9.1	12.4	7.8	9.4
LYM (%)	14.7	14.4	19.5	16.4	21.5	17.4
PLT (10^9/L)	262000	263000	294000	278000	313000	290000
ESR (мм/h)	63	62	40	44	17	26
hs-CRP (мg/dL)	32.5	32.5	17.2	18.5	0.7	2.5
AST (1/L)	83	81	57	61	31	43
ALT(1/L)	107	105	64	76	37	60
S-Fer (ng/mL)	1935.5	1932.0	1045.4	1103.5	433.9	559.5
GLU(mmol/L)	7.7	7.6	5.6	6.8	5.2	5.9

Table 4: Average clinical blood parameters of patients of both groups on the days corresponding to the 1st, the 4th and 10th THz irradiation procedures in the MG.

Indicators	The day corresponding to the 1st THz irradiation procedures in the MG		The day corresponding to the 4th THz irradiation procedures in the MG		The day corresponding to the 10th THz irradiation procedures in the MG	
	MG	CG	MG	KG	MG	KG
Sleep deprivation	6	6	3	4	0,5	2,5
Mood deprivation	7,5	7	4	5,5	1,5	3,5
Weakness	6.5	6	3,5	5	1,5	4
Dizziness	4	4	2	3	0.5	2
Decreased appetite	6	6	3	4	1	3
Headaches	7	7	5	6	1.5	3.5
Muscle pain, myalgia	8	8	5	6	2	4
Decreased working capacity	7	7	4	5	2	4

Table 5: The average patient's subjective symptoms assessment for both groups on the days corresponding to the 1st, the 4th and 10th THz irradiation procedures in the MG.

For the correct positioning of the non-contact infrared thermometer over the projection of the anatomical structures, before the THz-therapy procedure, it is necessary to palpate the right and left lobes of the thyroid gland and the isthmus between them, slightly tilting the head back. The set of AP and the normative indicators of the temperature of the MTAP test in healthy people are shown in table 6.

Where are: T_{aver} - average temperature; r-l - Temperature difference in paired points; T°C Merc - Temperature measured with a mercury thermometer in the right armpit.

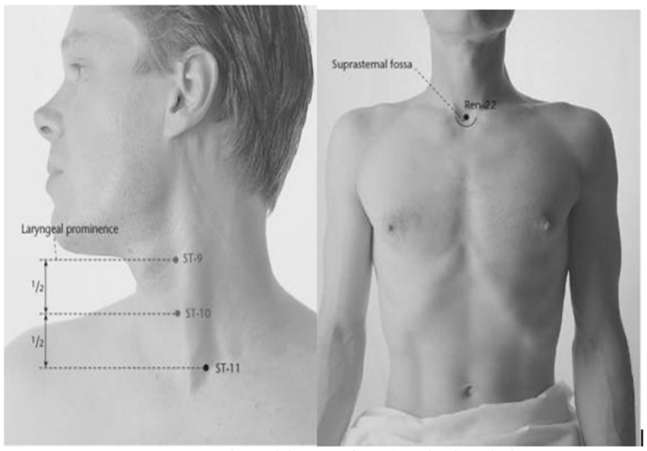

Figure 5: Acupuncture points Qishe (E11 / St11) (paired) and Tiantu (VC22).

To simplify temperature measurement in the AP RP21 for seriously ill patients, it is possible to measure the temperature with a non-contact infrared thermometer in the center of the armpit on the right and left, which, similar to the AP RP21 thermometry, allows to observe the course of rehabilitation processes.

The minimum and maximum values of the measured temperature in the AP Qishe (E11 / St11) and Tiantu (VC22) in MG patients before the start of THz therapy and at the end of the course are presented in table 7.

THz-therapy procedures were carried out in the morning to the area of the side with a higher temperature to the epicenters of AP Da-bao (RP21) (4-5 procedures, until the temperature difference decreases), and then to the epicenters of AP Qishe (E11 / St11) (paired) and Tyantu (VC22) 6-7 more procedures according to the same principle of increased temperature. At elevated temperatures in the isthmus of thyroid, the entire area of the gland was exposed.

During the research, it was found that the temperature indicators of the anatomical structures of the thyroid gland are important in assessing the dynamics of the course of complications of coronavirus infection and should be a reference point when conducting THz irradiation procedures in the form of a course application. Armpit body thermometry should be performed on both sides and the highest reading should be taken into account.

According to CT data, a regular course of the pathological process with positive dynamics was noted in both examined groups. However, it was found that THz irradiation is an important additional factor in the favorable outcome of coronavirus infection with complicated pneumonia. Considering different versions and trends of pharmacotherapy and intensive therapy methods, THz irradiation reduces side effects and promotes early recovery of patients at the stage of early rehabilitation. By the end of the THz-therapy course, the clinical and biochemical blood parameters in almost all patients with MG were within the normal range.

All of the above indicates the prospect of using the THz irradiation for therapy of pneumonia caused by coronavirus. Since coronavirus causes SARS, with a predominant lesion of the alveoli, exposure to the THz irradiation can stimulate the protein activity of the cell, activate its protective mechanisms, and also prevent the virion from joining the cell receptor. In addition, the THz irradiation results in the spin-dependent capture of oxygen to the iron ions in hem, thereby facilitating its transport and the corresponding blood oxygenation (scarlet blood) [10].

The use of THz Irradiation for an Early Diagnosis of Breast Disease

In order to better understand the characteristics of the transport of current carriers in the edge channels of the ultra-narrow quantum well, which forms the basis of the SNS, in particular, the Josephson effects, an experiment was conducted, where SNS was used as a recorder and source of THz irradiation. To register the THz response in this case, the identification of Shapiro steps under conditions of applying voltage in the plane of the quantum well and, in particular, along and across its edge channels, inside which the quantum spin-dependent carrier transport is implemented, was used [17]. Thus, a pair of SNS was used, one of them as a source, and the other as a recorder of THz irradiation. The Shapiro step when measuring the voltage on the U_{xx} (source-drain) contacts of the recorder arises as a resonance when it is irradiated with a SNS acting as a source, and the resonance is recorded by measuring the voltage change on the U_{xx} (source-drain) contacts of the recorder. In this case, the resonant response of the recorder is a consequence of a change in the electromagnetic field of the source: $h\nu = 2eU_{xx}$ [17]. During the experiment, the longitudinal current of the source-drain recorder was set, and a voltage drop was recorded at the contacts U_{xx}. Then, the stabilized source-drain current is changed in time, which represents also the source of an external electromagnetic field. Under these conditions, simultaneously with the switching on of the source current, a U_{xx} response arised, which seems to be analog the Shapiro step.

For THz cancer express diagnosis research we built a spectrometer with a SNS, built in the Hall geometry, used as a THz generator. During experiments current-voltage characteristics were measured. Device was aimed to the point of neoplasm localization. To find out correlations between reflection and/or emission properties of biotissue repeated measurement of the points remote from initial were conducted.

	Acupuncture points												ToC Merc
	VG20	VG14	VC4	Gi4 right	Gi4 left	RP21 right	RP21 left	F3 right	F3 left	Gi4 r-l	RP21 r-l	F3 r-l	
T_{aver}, oC	31,0	31,6	31,9	29,9	30,1	30,8	30,9	29,4	29,5	0,3	0,3	0,3	36,6
T_{min}, oC	29,2	29,1	29,8	27,3	27,5	28,9	28,7	27,8	27,9	0,0	0,0	0,0	36,2
T_{max}, oC	32,8	33,4	33,8	33,1	32,8	32,7	32,0	32,0	31,7	0,5	0,5	0,5	36,9

Table 6: Normal temperature of the MTAP test.

AP	T, oC Before THz therapy		T, oC After THz therapy		T, oC Normal	
	min	max	min	max	min	max
E11/St11 (right)	35.9	37.4	33.2	33.9	32.6	33.5
E11/St11 (left)	37.6	38.4	32.6	34.1	30.5	32.0
VC22	34.9	36.8	32.2	33.3	31.5	32.8

Table 7: The measured temperature in the AP Qishe (E11 / St11) and Tiantu (VC22) in MG patients before the start of THz therapy and at the end of the course.

Bio-tissue, in this case, performed as an emitter whereas SNS was a recorder of THz irradiation. By the other words, device operates as a balance recorder. I.e., current-voltage characteristics of the device carry information about bio-tissue properties which is shown in the dependence U_{xx} on the stabilized drain-source current interconnected with frequency (Figure 6).

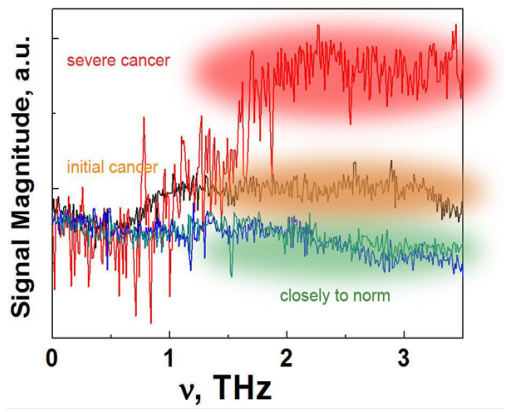

Figure 6: The THz response revealed by the conductance of the SNS which is obtained from the balance of radiation of biological tissue and SNS emitter. These spectral characteristics allow us to classify various pathological conditions of the tissue.

The dependence shows three different cases that correspond to different stages of oncology of the female breast. The control was carried out using ultrasound and high-resolution x-ray methods. It is clear that the signal power increases with the development of cancer. In addition to the contribution of the DNA oligonucleotide with frequencies of adenine (3.2 THz), guanine (2.9 THz), cytosine (2.7 THz) and thymine (2.5 THz) in the process of developing oncology, other features appear that indicate deterioration of the lymphatic system. Moreover, the phase of the local THz current-voltage characteristic is largely determined by the site of irradiation effect on the biological tissue. In addition, there is a characteristic change in the current-voltage characteristics in the region of one of the base frequencies (160 GHz), which reflects the operation of the lymphatic system. In particular, a change in the phase of the signal to a negative, as well as a shift of the peak to the frequency range of about 120 GHz, indicates an increasing activity of cancer. The observed analogous phase change in the IVC signal in the 3 THz region is interrelated with the patient's DNA structure, with carrier tunneling on adenine-thymine bonds. I.e., spectral characteristic represents human genome. A change in the phase of the signal on the resonant frequencies for the patient indicates an increasing activity of the tumor. It is a basis of more detailed THz diagnostics in future.

Summary

All of the above indicates the prospect of using the THz irradiation for medical applications both for therapy and for the diagnosis of various pathologies. It appeared that the IR - THz irradiation can be also applied to design the medical devices for the special therapy and prophylactics of different diseases, because the vast majority of the most important biochemical reactions in human body appear to be enhanced by optical pumping in this spectral range. "IR-Dipole", the device that has been constructed to bring these ideas to life generates a IR-THz irradiation in 1 – 700 mm wavelength range provided by the terahertz modulation frequency value from 40 GHz to 3.5 THz. The device has been developed using the different techniques within frameworks of the silicon planar nanotechnology.

But this is just a first step. What is needed next is an entire library of the unique THz signatures associated with every DNA oligonucleotide. That should be possible. This aim to start by analyzing the THZ resonance properties of each of the monomer and dimer molecules that make up oligonucleotides. The THz signatures from these should provide a kind of personalized medicine by creating individual THz chips for non-invasive control and constant correction of physiological parameters of the body: sugar level, etc. Similarly, such chips by frequency selection should control the characteristics of spin-dependent oxygen transport through iron ions in hemes, thereby repeatedly enhancing protective functions in pulmonary lesions regardless of the type of virus responsible for them.

Frequency selection in the terahertz range of the electromagnetic spectrum is able to lead to a controlled increase in intracellular and extracellular transport of proteins due to the controlled ATP GTP reaction (see[13]), thereby increasing the immune characteristics of the body, as well as - impeding the development of oncological diseases. Finally, today practically there are no technical and technological obstacles to the practical implementation of individual THz chips capable of performing the specified functions.

Acknowledgment

The work was carried out as part of a research program planned at affiliated organizations. No external funding was received for this study.

Compliance with Ethical Standards

All procedures performed in a study involving people comply with the ethical standards of the institutional and / or national committee for research ethics and the 1964 Helsinki Declaration and its subsequent changes or comparable ethical standards. Informed consent was obtained from each of the participants in the study.

References

1. Pickwell E, Cole BE, Fitzgerald AJ, Pepper M, Wallace VP (2004) *In vivo* study of human skin using pulsed terahertz radiation. Phys Med Biol 49: 1595 -1607.

2. Novoselov KS, Jiang Z, Zhang Y, Morozov SV, Stormer HL, et al. (2007) Room-Temperature Quantum Hall Effect in Graphene. Science 315: 1379.

3. Hasan MZ, Kane CL (2010) Colloquium: Topological insulators. Rev Mod Phys 82: 3045-3067.

4. Bagraev NT, Grigoryev VYu, Klyachkin LE, Malyarenko AM, Mashkov VA, et al. (2016) Room temperature de Haas - van Alphen effect in silicon nanosandwiches. Semiconductors 50: 1047-1054.

5. Bagraev NT, Chernev AL, Klyachkin LE, Malyarenko AM, Emel'yanov AK, et al. (2016) Terahertz Response of DNA Oligonucleotides on the Surface of Silicon Nanostructures. Semiconductors 50: 1208-1215.

6. Bagraev NT, Grigoryev VYu, Klyachkin LE, Malyarenko AM, Mashkov VA, et al. (2017) High-temperature quantum kinetic effect in silicon nanosandwiches. Low Temperature Physics/Fizika Nizkikh Temperatur 43: 132-142.

7. Taranets KB, Fomin MA, Klyachkin LE, Malyarenko AM, Bagraev NT, et al. (2019) Terahertz resonance response of biological tissue placed on a silicon nanostructure. J Appl Phys 125: 225702-225707.

8. Klinovaja J, Stano P, Yazdani A, Loss D (2013) Topological Superconductivity and Majorana Fermions in RKKY Systems. Phys Rev Lett 111: 186805-186805.

9. Zyuzin AA, Loss D (2014) RKKY interaction on surfaces of topological insulators with superconducting proximity effect. Phys Rev B 90: 125443-125445.

10. Bagraev NT, Klyachkin LE, Malyarenko AM, Novikov BA (2015) Medical application of terahertz silicon sources. Biotechnosphere 5: 55-70.

11. Kir'yanova VV, Zharova EN, Bagraev NT, ReukovAS, Loginova SV (2016) The prospects for the application of the electromagnetic waves in the terahertz frequency range for the purpose of physiotherapy. Russian Journal of Physiotherapy, Balneology and Rehabilitation 15: 209-215.

12. Chernev AL, Bagraev NT, Klyachkin LE, Emelyanov AK, Dubina MV (2014) DNA Detection By THz Pumping. Condensed Matter 10: 46:55.

13. Rothman JE, Orci L (1996) Budding vesicles in living cells. Sci Amer 274: 70-75.

14. Woodward RM, Cole BE, Wallace VP, Pye RJ, Arnone DD, et al. (2002) Terahertz pulse imaging in reflection geometry of human skin cancer and skin tissue. Phys Med Biol 47: 3853-3863.

15. Fischer BM, Walther M, Jepsen PU (2002) Far-infrared vibrational modes of DNA components studied by terahertz time-domain spectroscopy. Phys Med Biol 47: 3807-3814.

16. Reukov AS, Naymushin AV, Moroshkin VS, Kozlenok AV, Presnukhina AP (2017) The role of infrared irradiation with terahertz modulation in post-cardiosurgery pulmonary complications. Translational Medicine 4: 62-72.

17. Bagraev NT, Danilovskii EYu, Klyachkin LE, Malyarenko AM, Mashkov VA (2012) Spin Interference of Holes in Silicon Nanosandwiches. Semiconductors 46: 77-89.

Advances In Industrial Biotechnology | ISSN: 2639-5665

Advances In Microbiology Research | ISSN: 2689-694X

Archives Of Surgery And Surgical Education | ISSN: 2689-3126

Archives Of Urology

Archives Of Zoological Studies | ISSN: 2640-7779

Current Trends Medical And Biological Engineering

International Journal Of Case Reports And Therapeutic Studies | ISSN: 2689-310X

Journal Of Addiction & Addictive Disorders | ISSN: 2578-7276

Journal Of Agronomy & Agricultural Science | ISSN: 2689-8292

Journal Of AIDS Clinical Research & STDs | ISSN: 2572-7370

Journal Of Alcoholism Drug Abuse & Substance Dependence | ISSN: 2572-9594

Journal Of Allergy Disorders & Therapy | ISSN: 2470-749X

Journal Of Alternative Complementary & Integrative Medicine | ISSN: 2470-7562

Journal Of Alzheimers & Neurodegenerative Diseases | ISSN: 2572-9608

Journal Of Anesthesia & Clinical Care | ISSN: 2378-8879

Journal Of Angiology & Vascular Surgery | ISSN: 2572-7397

Journal Of Animal Research & Veterinary Science | ISSN: 2639-3751

Journal Of Aquaculture & Fisheries | ISSN: 2576-5523

Journal Of Atmospheric & Earth Sciences | ISSN: 2689-8780

Journal Of Biotech Research & Biochemistry

Journal Of Brain & Neuroscience Research

Journal Of Cancer Biology & Treatment | ISSN: 2470-7546

Journal Of Cardiology Study & Research | ISSN: 2640-768X

Journal Of Cell Biology & Cell Metabolism | ISSN: 2381-1943

Journal Of Clinical Dermatology & Therapy | ISSN: 2378-8771

Journal Of Clinical Immunology & Immunotherapy | ISSN: 2378-8844

Journal Of Clinical Studies & Medical Case Reports | ISSN: 2378-8801

Journal Of Community Medicine & Public Health Care | ISSN: 2381-1978

Journal Of Cytology & Tissue Biology | ISSN: 2378-9107

Journal Of Dairy Research & Technology | ISSN: 2688-9315

Journal Of Dentistry Oral Health & Cosmesis | ISSN: 2473-6783

Journal Of Diabetes & Metabolic Disorders | ISSN: 2381-201X

Journal Of Emergency Medicine Trauma & Surgical Care | ISSN: 2378-8798

Journal Of Environmental Science Current Research | ISSN: 2643-5020

Journal Of Food Science & Nutrition | ISSN: 2470-1076

Journal Of Forensic Legal & Investigative Sciences | ISSN: 2473-733X

Journal Of Gastroenterology & Hepatology Research | ISSN: 2574-2566

Journal Of Genetics & Genomic Sciences | ISSN: 2574-2485

Journal Of Gerontology & Geriatric Medicine | ISSN: 2381-8662

Journal Of Hematology Blood Transfusion & Disorders | ISSN: 2572-2999

Journal Of Hospice & Palliative Medical Care

Journal Of Human Endocrinology | ISSN: 2572-9640

Journal Of Infectious & Non Infectious Diseases | ISSN: 2381-8654

Journal Of Internal Medicine & Primary Healthcare | ISSN: 2574-2493

Journal Of Light & Laser Current Trends

Journal Of Medicine Study & Research | ISSN: 2639-5657

Journal Of Modern Chemical Sciences

Journal Of Nanotechnology Nanomedicine & Nanobiotechnology | ISSN: 2381-2044

Journal Of Neonatology & Clinical Pediatrics | ISSN: 2378-878X

Journal Of Nephrology & Renal Therapy | ISSN: 2473-7313

Journal Of Non Invasive Vascular Investigation | ISSN: 2572-7400

Journal Of Nuclear Medicine Radiology & Radiation Therapy | ISSN: 2572-7419

Journal Of Obesity & Weight Loss | ISSN: 2473-7372

Journal Of Ophthalmology & Clinical Research | ISSN: 2378-8887

Journal Of Orthopedic Research & Physiotherapy | ISSN: 2381-2052

Journal Of Otolaryngology Head & Neck Surgery | ISSN: 2573-010X

Journal Of Pathology Clinical & Medical Research

Journal Of Pharmacology Pharmaceutics & Pharmacovigilance | ISSN: 2639-5649

Journal Of Physical Medicine Rehabilitation & Disabilities | ISSN: 2381-8670

Journal Of Plant Science Current Research | ISSN: 2639-3743

Journal Of Practical & Professional Nursing | ISSN: 2639-5681

Journal Of Protein Research & Bioinformatics

Journal Of Psychiatry Depression & Anxiety | ISSN: 2573-0150

Journal Of Pulmonary Medicine & Respiratory Research | ISSN: 2573-0177

Journal Of Reproductive Medicine Gynaecology & Obstetrics | ISSN: 2574-2574

Journal Of Stem Cells Research Development & Therapy | ISSN: 2381-2060

Journal Of Surgery Current Trends & Innovations | ISSN: 2578-7284

Journal Of Toxicology Current Research | ISSN: 2639-3735

Journal Of Translational Science And Research

Journal Of Vaccines Research & Vaccination | ISSN: 2573-0193

Journal Of Virology & Antivirals

Sports Medicine And Injury Care Journal | ISSN: 2689-8829

Trends In Anatomy & Physiology | ISSN: 2640-7752